www.lajss.org
Latin American Journal of Solids and Structures 3 (2006) 21–39

Energy absorption and ballistic limit of targets struck by heavy projectile

M. Ganesh Babu[a], R. Velmurugan[a,*] and N. K. Gupta[b]

[a]COMPTEC, IIT Madras
[b]Dept of Applied Mechanics, IIT Delhi, India

Abstract

Impact on composite structures was a critical topic with great importance in the recent past. In this paper, impact on Glass/epoxy laminates by a 558.6 gms mild steel cylindro-conical projectile, in the range of 30 – 100m/s, was studied. Composite panels consisting of 3 and 5 layers of 3 types of glass reinforcement with different combinations were prepared viz.3 layers of WRM/epoxy, CSM/epoxy, Glass Fabric/epoxy, WRM/CSM/epoxy, WRM/Fabric/epoxy and CSM/Fabric/epoxy laminates. Tests were conducted to determine the ballistic limit as well as energy absorption for different initial velocity of the projectile using a piston type, gas gun launcher. A mathematical model based on the energy balance principle was proposed to predict the ballistic limit. The WRM/ epoxy laminates showed higher energy absorption capability and better ballistic limit whereas CSM/Epoxy showed the least of all. Increase in energy absorption was noted up to a certain limit and then decreases slightly for all the 6 types of panels. The delamination area increased with increase in initial velocity up to ballistic limit and a small decrement was observed from thereon. The ballistic limit determined experimentally was compared with the proposed model and showed good agreement with the experimental value.

Keywords: ballistic limit, glass reinforcement, and energy absorption and mathematical modeling.

List of symbols

Adel	Area of the delaminated zone
CSM	Chopped Strand Mat
d_f	diameter of the fiber
E	Young's Modulus
El	Energy lost by the projectile during impact
Etot	Total energy absorbed during an impact
Edef	Energy associated with global plate deflection

*Corresp. author Email: rvel@iitm.ac.in Received 15 October 2005; In revised form 12 December 2005

Edel	Delamination energy
Efrac	Fracture energy
Efric	Frictional energy
Ed	Energy density of the composite laminate
Ff	Frictional force
GIIc	Mode II interlaminar fracture toughness
h	Thickness of the laminate
ILSS	Interlaminar shear stress
Lp	Length of the projectile
M	Mass of the projectile
Rdel	Radius of the delaminated zone
R	Radius of the plate
R_p	Radius of the projectile
V	Initial velocity of the projectile
Vr	Residual velocity of the projectile
Vo	Ballistic limit
WRM	Woven Roving Mat
w_c	Central plate deflection
τ	Maximum shear strength
σ_r	Radial stress
ν	Poisson's ratio
σ_y	Yield strength of the composite
ε_r	Radial strain

1 Introduction

Fiber reinforced polymer matrix composites have been widely used in aerospace, marine and automotive structures due to their high specific strength, light weight and stiffness. But the main drawback with these materials is that they have poor impact resistance. They are susceptible to failure in the form of delamination when impacted by foreign objects. Impact damage in metal is easily detected as damage starts at the impacted surface; however, damage in composites often begins on the non-impacted surface or in the form of an internal delamination. The behavior of fiber reinforced composites when impacted by a solid object is the subject of much numerical, analytical and experimental research. The penetration and perforation of targets by projectile involve highly complex processes, which have been investigated experimentally for more than two centuries and analytically during the last two decades [1, 2].

Fiber reinforced laminates have been considered for armor application, glass fiber being more popular than other types of fiber such as kevlar because of their cost advantage [12]. Cantwell and Morton [4] studied the influence of projectile mass on CFRP laminates under low and high

velocity impact and found that low velocity impact results in global deformation whereas high velocity impact results in a localized deformation Information yielded by C-scans and optical micrographs indicated that, for a given impact energy, decreasing the impactor mass resulted in greater levels of incurred damage and, therefore, poorer post-impact properties. Fatt and Lin [9] studied the perforation of clamped woven E-glass polyester panels and proposed an analytical solution for a fully clamped panel under static indentation by a blunt cylinder. The analytical predictions of ballistic limit were within 13% of the test data, while the analytical predictions of total energy dissipated at the ballistic limit were within 25% of the test results. During impact, matrix cracking, delamination and fiber failure occurred and energy was absorbed in all these process. But most of the energy was absorbed in plate deflection and delamination, which reduced the panel bending stiffness and allowed higher transverse deformations to emanate away from the projectile. The more likely mode of failure for a laminated panel was large global plate deformation and tensile fracture [9].

Wen [11] investigated the penetration and perforation of FRP laminates using different shape of projectiles. Analytical equations were developed for predicting the penetration and perforation by projectiles with different nose shapes. It was based on the assumption that the deformation is localized and that the mean pressure offered by the laminate targets to resist the projectiles can be decomposed into two parts. One part is a cohesive quasi-static resistive pressure due to the elastic plastic deformation of the laminate materials. The other is a dynamic resistive pressure arising from velocity effects. It is shown that the model predictions are in good correlation with available experimental data.

Lee and Sun [8] carried out a combined experimental and numerical study of the dynamic penetration of clamped circular CFRP laminates by a 30g, 14.5 mm diameter flat ended projectile in the velocity range of 24 – 91 m/s. The material used was Hercules AS4 3501-6 graphite – fiber epoxy and the stacking sequence of all the laminates was based on a basic pattern, namely [0/95/45/-45]s. Three types of impact tests were conducted which had two thicknesses and the ballistic limits were determined. A finite element model was established to simulate the static punch process. It was shown that the computational results were in good agreement with the limited experimental data. Zhu et al [6] studied the response of kevlar/polyester laminate to quasi-static and dynamic penetration by cylindro-conical projectiles. Ballistic limit and terminal velocity were determined.

Most of the researchers have studied low and high velocity impact of projectiles on composite target. But the impact on composites in the velocity range of 30 – 100m/sec was given very less importance. This was critical in the case of automobiles, where the impact was likely to occur with in this range. In the present case, impacts on different composite targets were carried out to estimate the ballistic limit and energy absorption, based on which a mathematical model was proposed.

2 Experimental

2.1 Specimen preparation

Six sets (combination of WRM, CSM and Glass Fabric) of composite panels consisting of 3 and 5 layers were prepared by hand lay-up technique. Commercially available epoxy (Araldite LY556, Hardener HY951) was used as the matrix material. Chopped strand with 600 gsm and WRM with 610 gsm was used in the present study. Uniform thickness was maintained during manufacturing for each set of laminates. In case of combination of different reinforcement either CSM or fabric was placed in-between two WRM. A weight fraction of 50% (approximately 32% volume fraction) was maintained for all the laminates. The laminates were cured in room temperature and sufficient time was given for complete curing. The material properties were given in Table 1. The panels were cut to a size of 290 x 290 mm by a band saw cutter and the edges were trimmed. Sample specimens for static tests were cut from the same laminate so as to avoid any variation in mechanical properties.

Table 1: Material Properties of different lay-ups.

Material Property	WRM	Fabric	CSM	WRM/ Fabric	WRM/ CSM	CSM/ Fabric
Young's Modulus (E)	40.2	39.1	36.1	38.6	38.3	37.2
'GPa'	41.3	39	36.4	38.1	39.2	37.5
Average Panel	2.3	1.9	2.31	2.2	2.25	2.29
thickness (h) 'mm'	3.9	3.1	3.95	3.76	3.86	3.81
Poisson's ratio (ν)	0.3	0.3	0.29	0.3	0.29	0.29
	0.3	0.29	0.29	0.3	0.29	0.29
Interlaminar shear	17.44	15.26	15.2	16.2	15.23	15.2
strength ' N/mm^2'	20.36	16.23	18.3	20.1	17.23	16.23
Tensile strength of the	201	189	172	196	186	176
target (σ_y) 'MPa'	211	193	165	203	181	180
Energy Density (E_d)	11.1	10.2	8.63	10.9	10.9	9.6
'MPa'	15.6	11.6	9.23	12.1	11.3	10.8

2.2 Impact Test

Impact tests were performed on the composite panels using a piston type gas gun setup. The gun consists of a charging chamber, which has an inlet for charging, an outlet for releasing at one end and a provision to fit a 3.5m long barrel at its other end. The charging chamber was rested on two steel rails and pivoted at the center. A 2.5-m nozzle made of FRP was designed

and attached to the other end of the barrel in to which the projectile was placed. A stopper was attached to the FRP nozzle to prevent the projectile from getting into the steel barrel. A Projectile of mass 558.6gm made of mild steel was used in the experiment. The details of the projectile are given in the Table 2. Figure 1 show the experimental set up used to impact the composite specimens.

Table 2: Projectile Characteristics.

Characteristics	Projectile
Length of the Projectile (L_p)	100
Shank Length (L_s)	56
Nose Length (L_n)	44
Projectile Radius (R_p)	19.6
Mass (M)	556.8
Cone Angle (θ)	60°

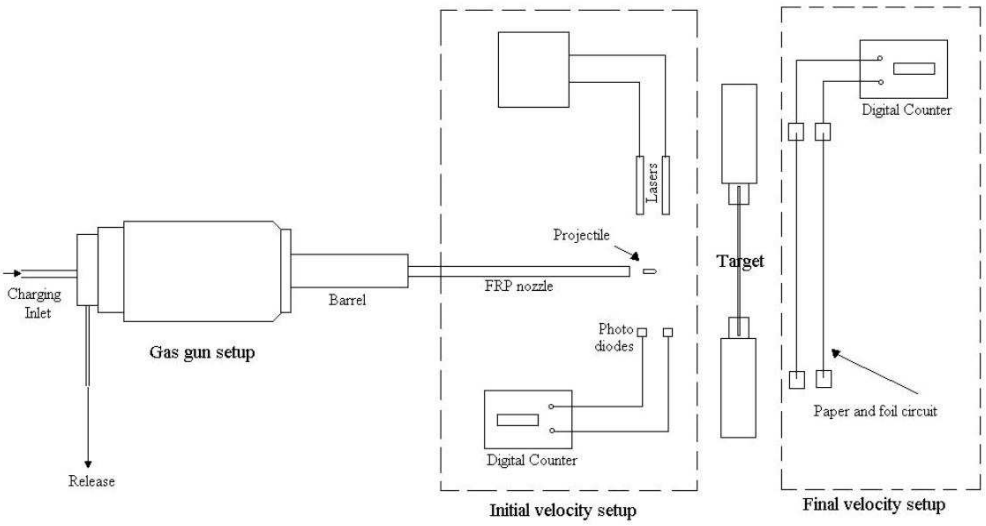

Figure 1: Experimental setup for conducting impact test

The specimen, which was prepared earlier, was mounted in the fixture and clamped on two opposite sides. The fixture was placed perpendicular to the direction of travel of projectile, at a distance equal to 1m from the end of the nozzle. This gap between the target fixture and the end of the nozzle was utilized to accommodate the setup for measuring the projectile's initial velocity. The projectile was placed inside the nozzle and was accelerated by opening the release valve electrically, after charging the charging chamber of the gas gun setup with

compressed air up to the required pressure. Initial velocity of the projectile was determined using a laser- photo diode setup consisting of a pair of laser emitting source and photodiodes. The two laser emitting sources were mounted on a fixture and separated by a small distance. When the projectile crossed the first laser beam, it triggered the digital counter and the counter was stopped when the projectile blocked the second beam. From the counter reading and from the distance between the two laser beams, the initial velocity of the projectile was calculated.

A simple technique was developed in the present investigation for the measurement of residual velocity. Since the path of the projectile was unpredictable after penetration, the measuring device must be able to cover a certain area and the debris should not falsely trigger it. As a result, two papers of 500mm x 500mm were used. A continuous strip of conducting aluminium foil was pasted on the paper in a zigzag fashion as shown in figure 2. The gap between the strips could be varied depending on the size of the projectile. The two ends of the foil were connected to a battery source, which in turn was connected to an electronic counter to form a closed circuit. These papers were placed behind the target and separated by a known distance. Once the projectile penetrated the target, it pierced the paper and opened the circuit there by triggering the counter. During medium velocity impact the possibility of the formation of debris cloud was less and hence this set up could produce a reliable result. From the counter, the time taken by the projectile to pierce the papers was noted. Sandbags were placed behind the fixture to capture the projectile. It should be noted that the velocity obtained from the counter could be the exact residual velocity, provided, the trajectory of the projectile was normal to the paper after penetrating the target. However, the projectile tends to deviate from its normal path and can make a maximum angle of θ_{max} with the normal. Hence an error term has to be included to account for the deviation in the path of the projectile after penetration.

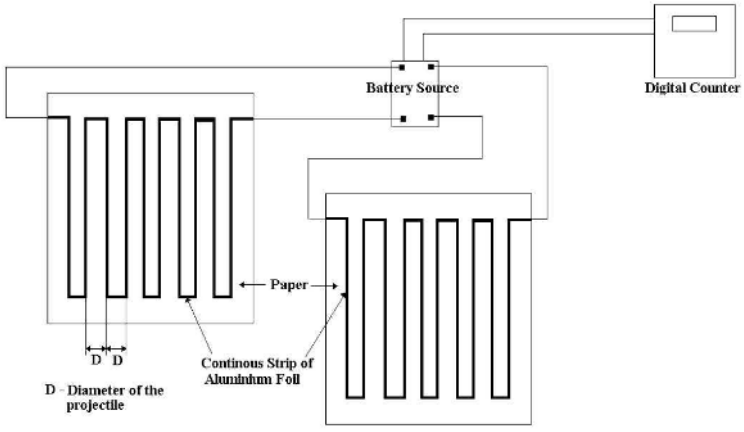

Figure 2: Setup to determine the residual velocity

The initial, final velocities and the corresponding kinetic energies of the projectile were calculated from the counter value and thus the energy absorption. After performing the impact test,

the surface and internal damages in the target were thoroughly analyzed. The delamination area was also visualized. This was repeated for all the specimens. The ballistic limit was determined experimentally by conducting the impact test at different initial velocity. The velocity at which the projectile got struck into the target was taken to be the ballistic limit.

2.3 Quasi-static test

Quasi-static tests were performed on the samples that were cut from the panels. Tensile strength, shear strength and flexural strength were determined using a Universal Testing Machine (UTM). Izod impact test was performed on the sample using Izod impact testing machine. Short beam test was performed to find out the shear strength using INSTRON UTM for the three different sets of laminates. The entire tests were carried out according to ASTM standards, samples of 5 were tested for each test and the average values were taken for analysis.

2.4 Analytical Modeling

An Analytical model is proposed to find out the ballistic limit of the target material. The model is based on the energy absorption principle. In developing the model, the following assumptions are made.

1. The projectile is rigid and remains undeformed during the impact. This is confirmed by experiment which showed that the projectiles retained their shape and mass after impact.
2. Projectile strikes the target normally.
3. There exist friction between the target and the projectile.
4. The failure mechanism of composites is uniform through out its thickness.
5. There is no change in volume during the impact.

The kinetic energy of a moving projectile of mass M, with a velocity V, is given by

$$K.E = \frac{1}{2}MV^2 \tag{1}$$

After striking the target, the velocity of the projectile becomes 'Vr'.

$$FinalK.E = \frac{1}{2}MV_r^2 \tag{2}$$

The energy lost during impact El is given by

$$E_l = \frac{1}{2}M\left(V^2 - V_r^2\right) \tag{3}$$

At ballistic limit the residual velocity is almost zero and hence the energy lost will be equal to the initial kinetic energy of the projectile.

$$E_l = \frac{1}{2} M V_0^2 \tag{4}$$

Where V_o is the Limiting velocity or ballistic limit, which is the velocity at which the projectile gets struck into the target and experimentally it can be taken as the average of three velocities just above ballistic limit and three below the ballistic limit.

During the medium or low velocity impact, the major portion of the energy is absorbed in global plate deflection or deformation as suggested by N.K.Gupta et al [7]. This can be seen from the experiment, where there is enough deflection of the target before perforation. Only after the deflection, delamination, fiber fracture and perforation have occurred, but the energy absorbed in global plate deflection is the major energy absorption process.

There is also evidence of delamination on the tested specimens, which absorbs a portion of the incident energy. In addition to this energy absorbing mechanism, there is some contribution from fiber failure, friction and fiber pull out.

Thus the total energy absorbed is given by

$$E_{tot} = E_{def} + E_{del} + E_{frac} + E_{fri} + E_{pull} \tag{5}$$

At ballistic limit this total energy absorbed is equal to the Energy lost by the projectile and hence

$$E_l = E_{tot} \tag{6}$$

$$E_{tot} = \frac{1}{2} M V_o^2 \tag{7}$$

$$\text{Ballistic limit} \qquad V_o = \sqrt{2E_{tot}/M} \tag{8}$$

In order to calculate the total energy absorbed during impact, the contribution of individual energies has to be evaluated.

3 Energy absorbed in global plate deflection

During medium velocity impact the deformation of the plate was assumed to be globalized. N.K.Gupta et al [7] have shown that the radial stretching of the plate absorbs major portion of the projectile energy during medium velocity impact for aluminium targets. This has been taken into consideration for our case also.

The energy of the radial stretching of the plate due to the radial stress σ_r is evaluated by neglecting the circumferential stress since radial stress is responsible for the radial cracks [3]

Strain energy can be written as

$$W = \int_v \left(\int \quad \sigma_r d\varepsilon_r + \sigma_\theta d\varepsilon_\theta \right) dv. \tag{9}$$

σ_r and σ_θ are the radial and circumferencial stresses and the corresponding strains are ε_r and ε_θ. Here the circumferencial strain is zero and neglecting the circumferencial Stress we get

$$W = \int_v \left(\int \quad \sigma_r d\varepsilon_r \right) dv. \tag{10}$$

Applying Mises Condition

$$\sigma_r^2 + \sigma_r \sigma_\theta + \sigma_\theta^2 = (\sigma_r + \alpha \varepsilon_r)^2 \tag{11}$$

Neglecting the work hardening 'α', we have

$$W = \frac{2\pi h}{\sqrt{1 - \nu + \nu^2}} \int_0^r \sigma_y . \varepsilon_r . r . dr \tag{12}$$

Where σ_y is the initial yield stress, h is the plate thickness and ν is the Poisson's ratio.
For large deflections, the radial strain can be approximately written as[11]

$$\varepsilon_r = \frac{1}{2} \left(\frac{dw}{dr} \right)^2 \tag{13}$$

$$W = \frac{2\pi h}{(\sqrt{1 - \nu + \nu^2})} \int \sigma_y \frac{1}{2} \left(\frac{dw}{dr} \right)^2 r . dr \tag{14}$$

It has been empirically found that permanent deformation profile of the plate subject to projectile impact is [10]

$$w(r) = w_o e^{-r} \tag{15}$$

$$W = \frac{\pi h}{\sqrt{1 - \nu + \nu^2}} \int \sigma_y . w_0^2 . e^{-2r} . r . dr \tag{16}$$

The lower limit was taken to be zero and the upper limit as the radius of the plate R. After integration, the Energy absorbed during plate deflection is found to be

$$E_{def} = \frac{\pi h \sigma_y . w_0^2 . (e^{-2R} . (1 + 2R))}{4 . \sqrt{1 - \nu + \nu^2}} \tag{17}$$

From the above expression it is possible to find out the energy absorbed during global plate deflection.

4 Energy absorbed in delamination

In the previous section, the energy absorbed during global plate deflection is calculated which is considered to be the major energy absorbing mechanism. There is also some contribution from delamination. The energy absorbed during delamination is given by [9]

$$E_{del} = A_{del}.GII_c \tag{18}$$

Here Adel is the area of the delaminated zone which can be calculated by

$$A_{del} = \pi R_{del}^2 \tag{19}$$

Where R_{del} is the radius of the delaminated zone, which can be given interms of the delamination load and interlaminar shear stress of the Glass/ epoxy.

$$R_{del} = \frac{P_d}{2\pi h(ILSS)} \tag{20}$$

Davis et all [5] used a simple mode II fracture analysis to describe the critical load for the onset of a single circular delamination in an isotropic material.

$$P_d^2 = \frac{8\pi^2 E.h^3.G_{II_c}}{9(1-\nu^2)} \tag{21}$$

Here E is the average panel stiffness that can be evaluated from the flexural test, ν is the Poisson's ratio

So the energy absorbed during delamination is given by

$$E_{del} = \frac{2EhG_{IIc}}{9(1-\nu^2)(ILSS)^2} \tag{22}$$

Where GII_c is the mode II interlaminar fracture toughness and ILSS is the interlaminar shear strength.

5 Energy absorbed in tensile fracture of the fibers

During the impact process, after plate deflection and delamination, the fibers under the point of impact undergoes tensile failure. There is also failure of the yarns along the crack length. The failure of yarn occurs when the deflection of plate reaches a maximum level. Beyond maximum deflection, the fibers under the point of impact undergo tensile failure due to radial stretching of the target. This tensile failure of the fibers has absorbed a portion of the incident energy.

If the energy density at the point of tensile fracture of the composite laminate per unit volume is Ed, (which can be approximately taken to be the area under the stress strain curve during tensile test) then the total energy absorbed in tensile fracture 'Efrac' is given by [5]

$$E_{frac} = E_d.V \tag{23}$$

V being the volume of the composite strained to its tensile failure. It has been experimentally found that, during impact, only the fibers under the point of impact have undergone tensile failure. Area of the composite, which has strained to tensile failure during impact by the projectile, is slightly greater than the area of the projectile. This can been seen from figure 3 and so the volume is treated to be equal to the volume of the composite with area equal to the cross sectional area of the projectile and the thickness equal to the thickness of the composite. The aim of the mathematical model is to predict the ballistic limit based on energy balance principle without carrying out dynamic test and so approximation such as this shows negligible effect.

$$E_{frac} = E_d.\pi R^2.h \tag{24}$$

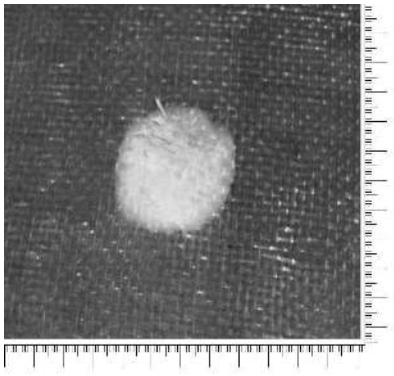

Figure 3: 5 layer WRM laminate showing no petals

6 Frictional Energy

In the previous investigations the energy associated with the friction between the projectile and the target has been neglected since the projectile was small. This is the case with high velocity impact. But with low and medium velocity impact some amount of energy is absorbed in overcoming the friction between the target and the projectile. More over when the mass and size of the projectile becomes large, the friction between the projectile and the target is more and hence this cannot be neglected. Energy associated with friction is given by

$$E_{fric} = F_f.L_p \tag{25}$$

Where F_f is the frictional force that can be evaluated from the static test and L_p is the length of the striker or the projectile.

The total energy is thus given by

$$E_{tot} = E_{def} + E_{del} + E_{frac} + E_{fric}$$

and the expression for ballistic limit is

$$V_o = \sqrt{2E_{tot}/M} \tag{26}$$

7 Results and Discussion

7.1 Crack and Petal formation

All the composite panels are tested with a cylindro -conical projectile. From the experiment it is found that the tested specimens show crack formation, which indicates that during impact, the plates have undergone radial stretching. Petals are not formed during impact on samples which contain WRM suggesting that WRM hinder the formation of petals during impact (figure 3). Since there are rovings in both the directions, it is difficult for the crack to break the rovings along a straight line leaving behind an irregular failure of the fibers. This phenomenon is observed in both 3 and 5 layered composite panels. But when CSM or Fabric is struck by projectile, petals are clearly seen. This can be confirmed from figures 4 and 5. In case of CSM, for velocity above ballistic limit, the number of petals was limited to 4 or 5 and the root of the petal was broken. Hence the friction is reduced between the target and the projectile. But in fabric/epoxy laminates, there are more than 5 petals and are of mostly triangular in shape and also the root does not fail.

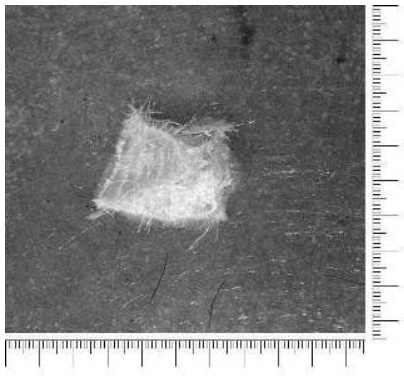

Figure 4: 3 layer CSM Laminate showing petals and crack

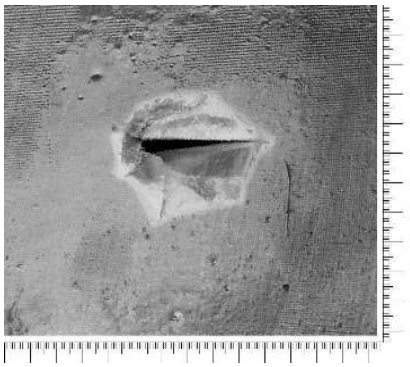

Figure 5: 5 layer Glass Fabric laminate showing petals and crack struck by projectile above ballistic limit

7.2 Perforation and Delamination

In all the tests performed, the geometry of the perforation matches exactly the shape of the projectile. But the area of delamination depends on both the projectile characteristics and nature of the target. Backlighting and visual inspection measure the area of delamination. It is almost equal for WRM, CSM and Fabric panels. Mostly the peripheral area around perforation and the area under impact are delaminated. The delamination area for a WRM/CSM and WRM/Fabric laminates are more when compared with other sets of 3 and 5 layer panels (Fig 6). This shows that when different types of reinforcement are used, the resulting composite panels are more susceptible to undergo large delamination during impact when compared to composites with similar type of reinforcement.

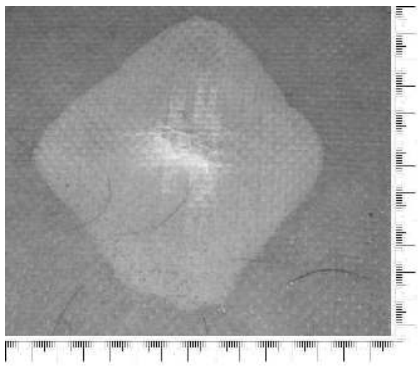

Figure 6: 5 layer WRM/CSM Laminate showing more delamination than other laminates struck by projectile below ballistic limit

Fig 7 shows the SEM picture of a WRM specimen struck by the projectile. The image is taken normal to the travel of projectile. It is seen that the bottom most ply has undergone more

delamination than the top most ply. It is also observed that there is good interfacial bonding between the fiber and the matrix. The crack runs in between the roving as well as between the layers. The lower most laminate has undergone stretching and subsequently underwent failure by the motion of the projectile. The damage pattern resembles the pine tree pattern as suggested by Abrate [1]. Extent of delamination is more on the rear side for all the tested panels and also the shape of the delaminated zone differs for the rear face. In some panels the delaminated zone is more or less circular in shape but with others it is of irregular shape. It is clear that the plate has undergone sufficient deformation, which absorbs major portion of the incident energy, before perforation and that tensile failure, has occurred on the back face of the laminate. When WRM or CSM or fabric alone is used, there is not much delamination in between the plies but when these are combined, an increase in delamination area is observed. The same failure pattern is also observed with 5-ply laminate.

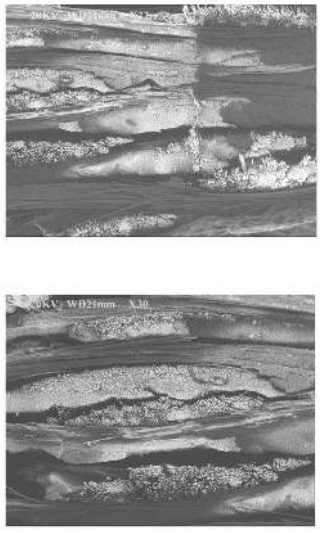

Figure 7: SEM Photographs of targets struck by cylindro conical projectile

7.3 Ballistic Limit

The ballistic limit for each target is determined from the experiment. For 3ply WRM laminates, the ballistic limit is approximately 35m/s whereas this limit is around 30m/s for CSM/WRM laminate, 27m/s for CSM laminates, 32m/s for Fabric, 33m/s for WRM/Fabric and 29m/s for CSM/Fabric laminates. For 5 layer laminates it is 39, 34, 31, 34, 35 and 32 m/sec, respectively. It is clear that WRM laminates possess higher ballistic limit amongst all. At lower velocities the perforation of the target does not take place but causes delamination and formation of circular rings (Figure 8) around the impact zone. These circular rings confirm the radial stretching of the target material during impact. It is also observed that at low velocities, more delamination

was seen on the lower most ply for all the laminates.

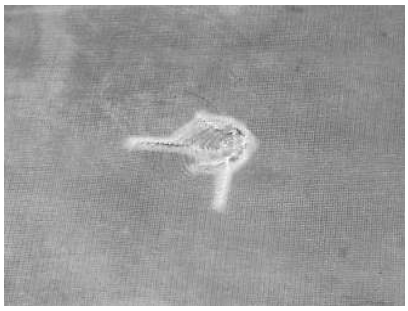

Figure 8: 3 layer Glass Fabric/Epoxy laminate showing the formation of concentric ring around the impact region

Figs 9 and 10 show the plot between the Initial velocity and the residual velocity for three and five layered laminates, respectively. From the figure it is clear that an increase in initial velocity results in the increase in residual velocity for all thickness. It is observed that the residual velocity remains zero up to a certain value of the initial velocity and then increases with the initial velocity. The velocity at which the residual velocity just shoots up may be treated as the ballistic limit. For WRM laminates more work is done to cause failure of the fiber and also more energy is spent in overcoming the friction between the panel and the projectile and hence more energy is absorbed showing higher ballistic limit. It is observed that increase in target thickness increases the ballistic limit irrespective of the nature of material.

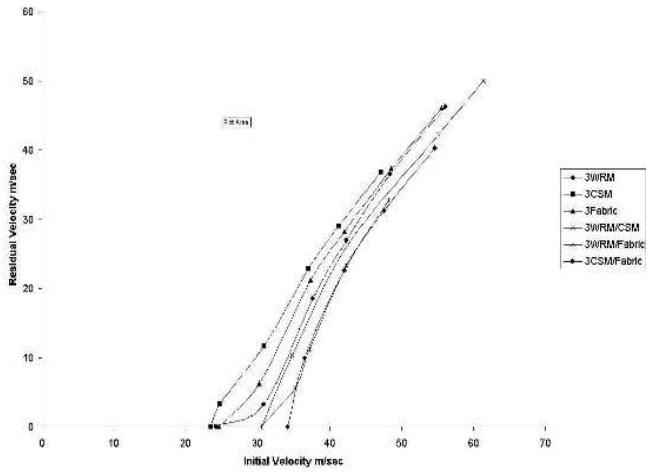

Figure 9: Initial Vs residual velocity for 3 layered laminates

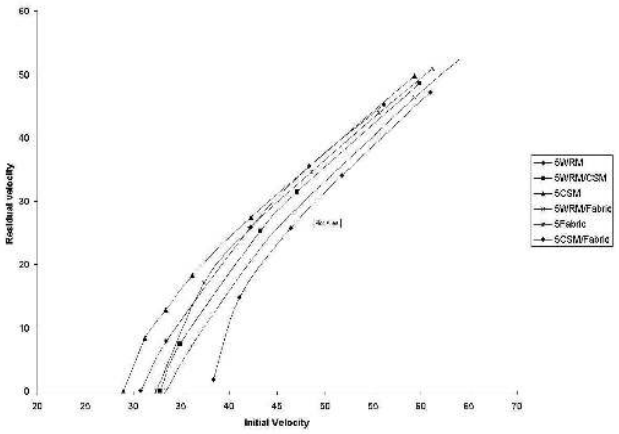

Figure 10: Initial Vs residual velocity for 5 layered laminates

7.4 Energy Absorption

Table 3 shows the energy absorbed by each process by a 3-ply laminate during impact. The incident energy is absorbed completely by the target until reaching the ballistic limit and beyond ballistic limit the energy absorbed increases for certain value of incident energy. As incident velocity increases further the energy decreases for all the laminates, as shown in Fig 11 and 12, which are the plots between initial velocity of the projectile and energy absorbed by each target. At velocities slightly above the ballistic limit, there is enough time for the target to undergo deflection, which is the major energy absorbing process. But at high velocities, the response time for the target is less and so the deflection of the target is less in comparison with the earlier case. This case is observed for all the laminates irrespective of thickness. Thicker laminates absorb more energy when compared to thin laminates. WRM/epoxy laminates absorb more energy when compared to other laminates. In such laminates, WRM laminate absorbs slightly higher energy than its counter part. These laminates absorb less energy than pure WRM laminates.

Table 3: Various Energies absorbed during impact on a 3 ply WRM laminate.

Energy absorbed in global plate deflection (E_{def})	150 Nm
Energy absorbed in delamination (E_{del})	45 Nm
Energy absorbed in tensile fracture of the composite (E_{frac})	35 Nm
Energy absorbed in friction between the projectile and the target (E_{fric})	95Nm
Energy absorbed in fiber Pull out (E_{pull})	8.6e-5 Nm
Total Energy absorbed (E_{tot})	329Nm
Ballistic Limit (predicted) V_b	34.6 m/sec.
Ballistic Limit (Experimental) V_b	36.2m/sec.

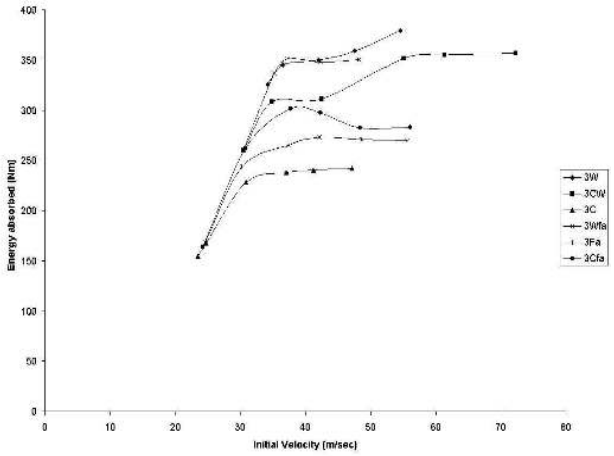

Figure 11: Energy absorbed by 3 ply laminates

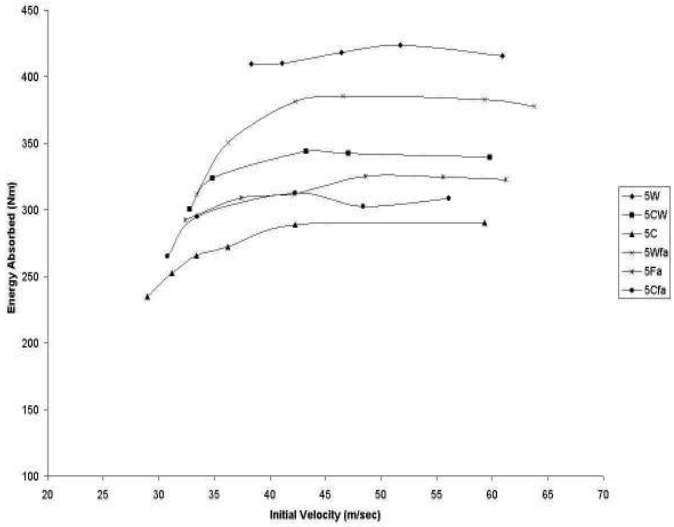

Figure 12: Energy absorbed by 5 ply laminates

7.5 Analytical Model

A mathematical model, based on energy balance principle is proposed to determine the ballistic limit. All the energy terms involved during the impact process are considered, calculated and equated to the initial kinetic energy of the projectile. The energy term associated with deflection is based on the assumption that only radial stress is responsible for deflection and the circumferential stress has negligible effect. For 3-ply WRM laminate, the experimentally

determined ballistic limit is approximately 35 m/sec. The predicted ballistic limit is found to be approximately 34 m/sec. It shows good correlation with the experimental value.

8 Conclusion

Impact tests were performed on different laminates between the range 30m/sec to 60m/sec, using a cylindro-conical projectile. The ballistic limit and energy absorption was calculated based on the experiment. It is found that the ballistic limit and the energy absorption are more for WRM laminates and CSM/Epoxy showed the least of all (35m/sec for 3 layers and 39 m/sec for five layers). Increasing the thickness by approximately 1mm increases the ballistic limit by approximately 6 m/sec. Increase in energy absorption was noted up to a certain limit and then decreases slightly for all the 6 types of panels. The delamination area increases when different reinforcements are used. Introduction of chopped strand mat and glass fabric does not improve the ballistic limit. The ballistic limit is predicted by analytical model and shows good agreement with the experimental value.

References

[1] S. Abrate. Impact on laminated composite materials. *Applied Mech Review*, 44(4):155–90, 1991.

[2] M.E. Backman and W. Goldsmith. The mechanics of penetration of projectiles into targets. *Int J of Engineering Science*, 16:1–99, 1978.

[3] C.A. Calder and W. Goldsmith. Plastic deformation and perforation of thin plates resulting from projectile impact. *Int. J. of Solids and Structures*, 7:863–881, 1971.

[4] W. J. Cantwell and J. Morton. The influence of varying projectile mass on the impact response of cfrp. *Composite Structures*, 13:101–114, 1989.

[5] G.A.O. Davis and X. Zang. Impact damage prediction in carbon composite structures. *Int. J. of Impact Engineering*, 16(1):149–170, 1995.

[6] Zhu G.Goldsmith and W. Dharan CKH. Penetration of laminated kevlar by projectiles-i. experimental investigation. *Int. J. of Solids and Structures*, 29(4):399–420, 1992.

[7] N.K. Gupta, R. Ansari, and S.K Gupta. Normal impact of ogive nosed projectiles on thin plates. *Int. J. of Impact Engineering*, 25(7):641–660, 2001.

[8] S-W Lee and R. Sun. Dynamic penetration of graphite/epoxy laminates impacted by a blunt-ended projectile. *Composite Science and Technology*, 22:561–88, 1993.

[9] S. Hoo Fatt Michelle, Duane M. Revilock Jr Chunfu Lin, and Dale A. Hopkins. Ballistic impact of glare fiber metal laminates. *Composite Structures*, 61:73–88, 2003.

[10] S.S.Morye et al. Modelling of the energy absorption by polymer composites upon ballistic impact. *Composites Science and Technology*, 60:2631–2642, 2000.

[11] H.M. Wen. Predicting the penetration and perforation of frp laminates struck normally by projectiles with different nose shapes. *Composite Structures*, 49:321–329, 2000.

[12] J.A. Zukus. Penetration and perforation of solids. In Zukus JA et al., editors, *Impact dynamics*, pages 155–214. Newyork: Wiley, 1982, 1982.